Aquaculture International
https://doi.org/10.1007/s10499-023-01129-0

Acute mortality of *Penaeus vannamei* larvae in farm hatcheries associated with the presence of *Vibrio* sp. carrying the *Vp*PirAB toxin genes

Pablo Intriago[1,2] · Andres Medina[3] · Jorge Espinoza[4] · Xavier Enriquez[4] · Kelly Arteaga[3] · Luis Fernando Aranguren[5] · Andrew P. Shinn[6] · Xavier Romero[3]

Received: 8 December 2022 / Accepted: 27 April 2023

Abstract
High and sudden mortalities of *Penaeus vannamei* post-larvae stage 1+ in Latin American hatcheries are attributed to a species of *Vibrio* carrying *Vp*PirAB genes. Mortalities occasionally occurred within 2 h from presenting a normal appearance to experiencing 100% mortality. This study analyzed historical samples of diseased and healthy *P. vannamei* from commercial shrimp hatcheries that had experienced sudden and significant mortality rates, to investigate the matter. Post-larvae samples (PL1–PL5) of *P. vannamei* were collected from a total of 22 tanks located in six distinct commercial shrimp hatcheries in Latin America that had reported occurrences of mortality among their shrimp. The samples underwent microbiological, molecular-biological, and histopathological analyses. Histopathology revealed massive sloughing and detachment of hepatopancreocytes. Disease progression can be categorized into two phases: an early phase characterized by a light infiltration of hemocytes prior to the sloughing of cells, followed by the acute-terminal phase where there is massive sloughing of hepatopancreatic epithelial cells, necrosis, a loss of hepatopancreatic architecture, cell debris in the lumen, and the loss of the peritrophic membrane. The rapid onset and progression of the early phase is frequently missed and, in most cases, was difficult to observe; the subsequent pronounced hepatopancreatic infiltration of hemocytes, massive sloughing, and absence of the peritrophic membrane can be used as an indication that a similar pathology is present. Molecular studies in combination with histological evidence are needed to confirm disease etiology. This condition is tentatively termed as post-larvae acute hepatopancreatic necrosis disease (PL-AHPND) to differentiate this from other pathologies affecting post-larval shrimp.

Keywords PirAB · *Vibrio* · AHPND · Post-larval shrimp · *Penaeus vannamei* · Farm hatchery

Handling Editor: Brian Austin

✉ Pablo Intriago
pintriago@southfloridafarming.com

Extended author information available on the last page of the article

Introduction

Since the advent of shrimp farming in the 1970s, commercial hatchery production has needed to expand rapidly to accommodate the demand for post-larvae. The lack of appropriate biosecurity measures during this expansion has, however, left the industry vulnerable to infections from viruses, bacteria, and fungi (Lightner 1996; Garibay-Valdez et al. 2020). Infections caused by *Vibrio* species are the primary bacterial diseases that pose a challenge to shrimp production, and they have been identified as the root cause of these syndromes and illnesses. Failure to address these infections can lead to high mortality rates, as reported in studies such as Baticados et al. (1990), Lavilla-Pitogo et al. (1990), Karunasagar et al. (1994), Morales-Covarrubias et al. (2018), and Zou et al. (2020). Various health conditions caused by *Vibrio* have been reported, including "bolitas syndrome" in zoea 2 caused by *V. alginolyticus*, *V. campbellii*, *V. harveyi*, *V. mimicus*, and *V. parahaemolyticus* (see Soto-Rodríguez et al. 2006a, b; Cuéllar-Anjel et al. 2014; Kumar et al. 2017); septic hepatopancreatic necrosis (SHPN) with or without luminescence caused by *V. alginolyticus*, *V. campbellii*, *V. harveyi*, *V. parahaemolyticus*, *V. penaeicida*, and *V. vulnificus* (see Morales-Covarrubias and Gómez-Gil 2014; Stern and Sonnenholzner 2014; Morales-Covarrubias et al. 2018); and glass post-larvae (GPD) or translucent post-larvae disease (TPD) caused by *V. parahaemolyticus* (see Zou et al. 2020). A review of these diseases and their etiological agents can be found in de Souza Valente and Wan (2021).

Interestingly, all these epizootics impact the health and normal functioning of the hepatopancreas. Zoea 2 syndrome aka "bolitas syndrome" is characterized by high mortalities of stock 36–48 h after the metamorphosis from zoea 1 to zoea 2. Following cell detachment of hepatocytes ("bolitas"), the "bolitas" can be seen traveling along the intestine; animals experience anorexia, a rapid evacuation of intestinal contents, and lethargy coupled with bouts of erratic swimming (Robertson et al. 1998). Zoea 2 syndrome described from shrimp hatcheries in India is reported to have a pathology that also includes impacts to the hepatopancreas with sloughing of the hepatopancreatic epithelial cells (Kumar et al. 2017).

Green luminescence in juvenile stock is characterized by the presence of luminescent *Vibrio*, the presence of bacterial colonies in the lumen of the hepatopancreatic tubules, hemocyte infiltration, and hemocytic nodules in the appendages, digestive tract, intestines, and hepatopancreas (Vandenberghe et al. 1998).

Shrimp affected by septic hepatopancreatic necrosis can display empty intestines, erratic swimming, organic matter accumulation in the gills, and melanization and necrosis of the appendages and cuticle. Hemocytic infiltration forming nodules around the affected hepatopancreatic tubules can be observed with H&E staining. Some nodules show melanization. The presence of bacteria is common. Other *Vibrio* spp. infections can also affect different organs, such as the heart, gills, lymphoid organ, antennal gland, tissue and nerve cord, connective tissue, telson, stomach, esophagus, appendages, muscle, and hepatic cecum, as documented by Lightner (1996).

"Translucent post-larvae disease" (TPD) or "glass post-larvae disease" (GPD) of *P. vannamei* is characterized by a pale or colorless hepatopancreas and digestive tract. A highly virulent strain of *V. parahaemolyticus* has been isolated from China and is the cause of TPD. *Vibrio parahaemolyticus* causing TPD, however, differs from the strains that have resulted in acute hepatopancreatic necrosis disease (AHPND) (Zou et al. 2020). Histopathological analysis of diseased samples indicated that these strains caused severe necrosis and sloughing of epithelial cells of the hepatopancreas and midgut in shrimp individuals both naturally and experimentally infected (Zou et al. 2020; Yang et al. 2022).

AHPND caused typically by pathogenic isolates of *V. parahaemolyticus* carrying the virulence plasmid and that codes for the Pir-toxin has resulted in significant economic losses to the shrimp industry, principally during the early part of grow-out production in ponds (Tran et al. 2013; Shinn et al. 2018; Prachumwat et al. 2019; Tang et al. 2020). AHPND known colloquially within the farming community as "early mortality syndrome (EMS)" generally occurs within the first 20 to 30 days of pond culture that can result in mortalities of up to 100% in affected populations (Tran et al. 2013; Santos et al. 2020). AHPND has been found in Asia as well as in the Americas (Santos et al. 2020). *Vibrio parahaemolyticus*, *V. campbellii*, *V. owensii*, *V. punensis*, and a strain close to *V. harveyi* have all been shown to harbor the pVA-1-type plasmid causing AHPND (see Dong et al. 2017; Dong et al. 2019; Santos et al. 2020). Other *Vibrio* bacteria including *V. campbellii* (see Han et al. 2017), *V. harveyi* (see Kondo et al. 2015), *V. owensii* (see Xiao et al. 2017), and *V. punensis* can carry these pathogenic plasmids (Restrepo et al. 2018). pVA1-like plasmids contain two genes for AHPND's main virulence factors which are PirA and PirB toxins (Han et al. 2015; Xiao et al. 2017). Temperature and salinity have been shown to affect PirA gene expression and regulate virulence (López-Cervantes et al. 2021).

The main histopathological feature of AHPND is that during the early to middle stage of the infection, there is sloughing and massive rounding of hepatopancreatic tubule epithelial cells but no detectable causative pathogen. Also, there is a characteristic medial to distal dysfunction of B (blister-like), F (fibrillar), and R (resorptive) cells, prominent karyomegaly, and a lack of mitotic activity in E cells (Tran et al. 2013). In contrast to this, the final stages of infection can be characterized by a huge aggregation of hemocytes and emergence of melanized granulomas, accompanied by an infection of many bacterial colonies of different types in the lumen of tubules. These late manifestations in infected shrimp cannot be easily distinguished from other serious and conventional infections brought about by non-AHPND isolates of various bacterial species (Tran et al. 2013). This is supported by the recent report regarding the histopathology of chronic survivors of previous AHPND events (Aranguren et al. 2020).

Since 2015, several different shrimp hatcheries in Latin America have reported outbreaks of sudden and acute mortalities during the larval rearing phase of production. The outbreaks typically occur over a period of 2 h (*pers. obs*.). The condition of the larvae, usually starting at post-larvae 1 (PL1), changes from an active and apparently healthy state to moribund and dead. The speed and virulence at which these massive mortalities have occurred have been observed in many laboratories (*pers. obs*.). Traditional disinfections and dry-out periods appear to be insufficient as many hatcheries report continuous outbreaks, sometimes up to four continuous cycles. This has resulted in recommendations surrounding the use of stronger concentrations of disinfection agents and extended dried-out periods.

To investigate this, the current study analyzed historical samples of diseased and moribund shrimp as well as healthy animals from commercial shrimp hatcheries that had reported sudden and high rates of mortality. All samples were analyzed using a combination of histopathology, PCR, and microbiology to determine the origin of these mortalities.

In the present study, we provide evidence to demonstrate that the cause of these mortalities was a *Vibrio* sp. bacterium carrying the same plasmids as the Vp_{AHPND} reported causing AHPND in culture ponds elsewhere. The condition is tentatively named post-larvae AHPND (PL-AHPND) to differentiate it from other pathologies affecting penaeid shrimp larvae.

Materials and methods

Sample collection

Samples of *Penaeus vannamei* originating from six different commercial shrimp hatcheries in Latin America (details withheld due to confidentiality) throughout a period spanning August 2015 until May 2021 were analyzed. Approximately 4 g of PL (i.e., ca. 1500 PL) at stages ranging from PL1 to PL5 from a total of 22 different tanks were collected. The affected tanks were those that showed white animals, without food in the intestine and with mortality. Larvae from non-affected tanks were taken simultaneously as controls. Additional samples were taken from shrimp farms and hatcheries within the same area to compare between sites (details withheld due to confidentiality).

Histopathology

From the sample of post-larvae taken from each tank (approximately 1500 post-larvae), more than half of the animals (i.e., 750+) were subsequently fixed in Davidson's AFA (i.e., alcohol, formalin, acetic acid) for 24 h and then processed for routine histology; i.e., 5-µm-thick sections were cut and stained with hematoxylin and eosin (H&E) following the procedures outlined by Bell and Lightner (1988). From each tank, 4 tissue sections were cut from each paraffin block; each paraffin block contained approximately 35 to 50 PL. The percentage of larvae that presented histopathological changes such as infiltration of hemocytes or sloughing of tissue was calculated from the total number of larvae examined in all the paraffin sections examined for each case.

Molecular biology

DNA extraction

One gram of shrimp larvae (approximately 400 PL) was fixed in 90% alcohol and used for PCR analysis. Bacteria DNA was extracted using an Omega (Bio-Tek) E.Z.N.A.® Tissue DNA kit following the manufacturer's guidelines. In brief, each sample of PL was minced with sterilized scissors and then ground using a microcentrifuge pestle. About 30 mg of shrimp was then moved to a clean 1.5-mL Eppendorf tube. To this, 200 µL of tissue lysis buffer (TL) and 25 µL of Omega Bio-Tek (OB) protease solution were added, and the mixture was vortexed and then incubated at 55 °C for approximately 3 h with vortexing every 30 min. RNA was removed by adding 4 µL of RNase A (100 mg/mL), and after mixing, the sample was kept at room temperature for 2 min. The sample was then centrifuged at 13,500 rpm for 5 min, and the supernatant was carefully transferred to a new 1.5-mL Eppendorf tube. To this, 220 µL of BL buffer was added, and the mixture was vortexed and incubated at 70 °C for 10 min. Next, 220 µL of 100% ethanol was added, and the mixture was vortexed; the contents were passed through a HiBind® DNA Mini Column into a 2-mL collection tube. The columns were then centrifuged at 13,500 rpm for 1 min, and the filtrate was discarded. Subsequently, 500 µL of HBC buffer (diluted with 100% isopropanol) was added to the column, and the sample was spun at 13,500 rpm for 30 s. The filtrate was discarded, and the column was washed twice with 700 µL of DNA wash buffer diluted with 100% ethanol, and

the sample was spun at 13,500 rpm for 30 s. The filtrate was discarded. This wash step was repeated. The column was then centrifuged at 13,500 rpm for 2 min to dry it out. The dried column was placed in a new nuclease-free 1.5-mL Eppendorf tube, and 100 µL of elution buffer, which was heated to 70 °C, was added to the column. The sample was allowed to sit for 2 min before being centrifuged at 13,500 rpm for 1 min. This elution step was repeated. The eluted DNA was then stored at – 20 °C until needed.

AP4 nested PCR method for the detection of VpPirAB genes

PirAB toxin genes in both larvae and in all the presumptive *Vibrio* spp. isolated were assayed using the nested AP4 method of Dangtip et al. (2015) and the OIE manual (2019), Chapter 2.2.1. In brief, the samples were prepared in a volume of 25 µL with 2 µL of DNA template (50–100 ng/µL), 12.5 µL of DreamTaq Green PCR Master Mix (2×) (Thermo Scientific™), 0.5 µL of 10 µM AP4-F1 (5′-ATGAGTAACAATATAAAACATGAAAC-3′), 0.5 µL of 10 µM AP4-R1 (5′-ACGATTTCGACGTTCCCCAA-3′), and 9.5 µL of nuclease-free water. The samples were subjected to PCR using a ProFlex™ 3×32-well–GeneAmp 9700 cycler (Thermo Fisher Scientific), which involved an initial denaturation step of 2 min at 95 °C, followed by 30 cycles of denaturation for 30 s at 95 °C, annealing for 30 s at 55 °C, and extension for 90 s at 72 °C, and a final extension step of 2 min at 72 °C. Then, a second PCR was performed using 2 µL of the first PCR product and the same volumes of other reagents except for 0.375 µL of 10 µM AP4-F2 (5′-TTGAGAATACGGGACGTGGG-3′) and 0.375 µL of 10 µM AP4-R2 (5′-GTTAGTCATGTGAGCACCTTC-3′). The second PCR involved an initial denaturation step of 2 min at 94 °C, followed by 25 cycles of denaturation for 20 s at 94 °C, annealing for 20 s at 55 °C, and extension for 20 s at 72 °C, and a final extension step of 2 min at 72 °C.

Detection of antibiotic resistant genes by conventional PCR

In addition, all presumptive *Vibrio* strains were tested for the presence of toxR, tet(A), tet(B), tet(C), tet(D), tet(E), and tet(G) genes by conventional PCR following the methodology given by Aguilera-Rivera et al. (2019); this was conducted to determine if antibiotic resistant genes were associated with the pathogenic strains. The testing of each sample was performed using a 25-uL reaction containing 2 µL of DNA sample, 12.5 µL of DreamTaq Green PCR Master Mix (2×) (Thermo Scientific™), 0.5 µL of each gene-specific forward and reverse primers (as listed in Table 1), and 9.5 µL of nuclease-free water. The PCR was conducted using a ProFlex™ 3×32-well–GeneAmp 9700 cycler (Thermo Fisher Scientific). The amplification conditions for toxR involved an initial denaturation step at 94 °C for 5 min, followed by 30 amplification cycles consisting of denaturation at 94 °C for 1 min, alignment at 58 °C for 1 min, and extension at 72 °C for 1 min. For tet(A), tet(B), tet(C), tet(D), tet(E), and tet(G), the amplification conditions were an initial denaturation step at 94 °C for 3 min, followed by 30 amplification cycles consisting of denaturation at 94 °C for 30 s, alignment at 55 °C for 30 s, and extension at 72 °C for 30 s.

Microbiology of the larvae

The total concentration of bacteria in the larvae was determined by first bathing the larvae (i.e., 1 g or approximately 400 PL9) held in a 500-µm nylon sieve for 5 min in a solution of 50 ppm active chlorine made up with 35 ppt seawater and then rinsed with excess sterile seawater. The larvae were weighed using a digital balance (Mettler) accurate to 0.01 g and

Table 1 The PCR primers used in the study

Pathogen/genes	Name	Sequence	Size, bp	Ref
AHPND	AP4-F1	ATGAGTAACAATATAAAACATGAAAC	1269	1
	AP4-R1	ACGATTTCGACGTTCCCCAA		
	AP4-F2	TTGAGAATACGGGACGTGGG	230	
	AP4-R2	GTTAGTCATGTGAGCACCTTC		
Genes	toxR	5′-GAAGCAGCACTCACCGAT-3′	382	2
		5′-GGTGAAGACTCATCAGCA-3′		
	tet(A)	5′-GCGCTNTATGCGTTGATGCA-3′	387	
		5′-ACAGCCCGTCAGGAAATT-3′		
	tet(B)	5′-GCGCTNTAGCGTTGATGCA-3′	171	
		5′-TGAAAGCAAACGGCCTAA-3′		
	tet(C)	5′-GCGCTNTATGCGTTGATGCA-3′	631	
		5′-CGTGCAAGATTCCGAATA-3′		
	tet(D)	5′-GCGCTNTATGCGTTGATGCA-3′	484	
		5′-CCAGAGGTTTAAGCAGTGT-3′		
	tet(E)	5′-GCGCTNTATGCGTTGATGCA-3′	246	
		5′-ATGTGTCCTGGATTCCT-3′		
	tet(G)	5′-GCGCTNTATGCGTTGATGCA-3′	803	
		5′-ATGCCAACACCCCCGGCG-3′		

1 = Dangtip et al. (2015), 2 = Aguilera-Rivera et al. (2019)

then placed in a mortar with approximately 1 g of autoclaved beach sand and 10 mL of sterile seawater which was used to facilitate the grinding of the bulk of larvae. Once the sample had been ground, the volume and weight were recorded again, then the samples were sequentially diluted in test tubes with sterile seawater to 1×10^2, 10^3, and 10^4. Then, 100 µL of the relevant dilution was placed on Petri dish plates containing either tryptic soy agar (TSA, Difco), thiosulfate-citrate-bile-sucrose agar (TCBS, Difco), or CHROMagar™ *Vibrio* and then incubated for 24–48 h at 30 °C. Thereafter, the number of colony-forming units (CFU) on each plate was recorded. Dilutions were based on obtaining > 20 to < 200 colonies per plate. Bacteria were also isolated and then enriched by picking 10 colonies from an overnight culture in TSA (30 °C). Identification of bacteria was performed using an API 20E Kit (Buller 2004).

LC50 studies

Live samples of different stages of *P. vannamei* larvae taken from a local hatchery (i.e., PL1–2, PL3–4, and PL9–10) and were placed (i.e., 10 larvae of each PL stage per flask) in 250-mL flasks containing 100 mL media, for each bacterial concentration under evaluation. Five replicates were used in each experiment. The medium was composed of 95% full-strength (35 ppt) seawater with 5% of culture of the centric diatom *Thalassiosira weissflogii* (Bigelow Laboratory). The final average cell concentration of the diatoms ranged from 6000 to 7000 cells per milliliter. This was done to mimic the culture conditions in hatchery tanks and to provide a food source for the larvae during the experimental trials.

The LC50 trials were conducted at two temperatures of 30 °C and 34 °C over a period of 24 h. The flasks were placed in a microbiological incubator (LABTOP) fed with a source of light (Silvana 50-W LED bulb). Light intensity was recorded using a LI-COR (model LI-1500-UW); av. reading was 2.83 µmol/m^2 s. Five concentrations of a *V. parahaemolyticus*-AHPND positive strain "Vp + 418" were tested, i.e., 0 (control), 10^3, 10^4, 10^5, and 10^6 CFU per milliliter. The Vp + 418 strain was isolated from a local outbreak of AHPND in 2016 and characterized by API (see Table 2). Vp + 418 were grown overnight in a shaker using tryptic soy broth (TSB) with half-strength seawater (16 ppt) at 30 °C at 100 rpm; cells were harvested by centrifugation at 10,000 × g for 15 min, rinsed with sterile seawater, and re-suspended with sterile seawater before adding the desired concentration into each flask. The bacteria were rinsed in sterile seawater to avoid the transfer of toxins generated during the flask culture. The density of the bacteria was determined by epifluorescent microscopy using acridine orange (Hobbie et al. 1977) and Sybr Green (Noble and Fuhrman 1998).

Results

Histopathology

Samples of post-larvae were collected from each of the control tanks ($n = 11$; throughout 2015–2021), with the sample size ranging from 16 to 108 post-larvae per tank. The PL sampled from these tanks presented normal histology of the hepatopancreas with an abundance of lipids, normal structural integrity of the tissue (Fig. 1a), and the presence of a well-defined peritrophic membrane in the intestine surrounding fecal material (Fig. 1b).

The post-larvae sampled from ten of the 11 "affected" tanks displayed typical AHPND lesions with a prevalence of between 8 and 97%. Prevalence was calculated by counting the total number of post-larvae within the tissue sections and then by dividing the number of disease-affected sections by the total number of post-larvae examined from a total of four tissue sections per case. In those cases, two clear phases were observed. The first phase was a mild to moderate hemocytic infiltration in the hepatopancreas tubule cells with the presence of a few sloughed cells in the hepatopancreas lumen. The percentage of this infiltration depended on the timing of when the post-larvae were sampled and the onset of the mortality event; the observed infiltration rate ranged from 5 to 20% (Fig. 1c, d). The remaining samples processed from the "affected" tanks displayed the typical acute phase of AHPND infection characterized by severe sloughing of the hepatopancreas tubule cells (Fig. 2a–d).

Figure 2 shows samples of post-larvae displaying the acute phase characterized by a severe sloughing of hepatopancreatic tubule cells in the hepatopancreas (Fig. 2b, d). At this stage, hemocytic infiltration is present in the hepatopancreas inter-tubular space, accompanied with moderate to massive epithelial cells sloughing into the lumen of several tubules (Fig. 2b–d).

The progression of necrosis and cell sloughing in the tubules of the hepatopancreas, in some cases, was so rapid that the only histopathological observations were the presence of sloughed cells in the lumen of the tubules and very little evidence of infiltrating hemocytes in affected areas (Fig. 2b, d). At this stage, there was a lack of peritrophic membrane and the presence of sloughed cells in the intestine (Fig. 2a). Melanosis was never present in any of the larvae that were examined, confirming the rapid onset of the AHPND infection.

Table 2 The characterization of bacteria isolated from sites reporting rapid rates of *Penaeus vannamei* larval mortality approximating PL-AHPND. The bacteria were characterized using a combination of physical features of the bacterial colonies, PCR testing, and biochemical testing by API 20E

Strains[a]	Origin	Luminescence[b]	PCR[c]								Microbiology		API 20E	
			AHPND	tox(R)	tet(A)	tet(B)	tet(C)	tet(D)	tet(E)	tet(G)	Color		Bacterial ID	%
											TCBS	CHROMagar[d]		
Tec5 (2021)	Hatchery	−	+	−	−	−	−	−	−	−	Yellow	White	*V. alginolyticus*	91.2
Tec8 (2021)	Hatchery	−	+	−	−	−	−	−	−	−	Yellow	White	*V. alginolyticus*	91.2
Tec4 (2021)	Hatchery	−	+	−	−	−	−	−	−	−	Green	Purple	*V. parahaemolyticus*	99.4
Tec6 (2021)	Hatchery	−	+	−	−	−	−	−	−	−	Green	Purple	*V. parahaemolyticus*	99.4
Tec7 (2021)	Hatchery	−	+	−	−	−	−	−	−	−	Green	Purple	*V. parahaemolyticus*	99.4
Sem1(2021)	Hatchery	+	+	−	−	−	−	−	−	−	Yellow	White	*V. alginolyticus*	85.9
Sem3(2021)	Hatchery	−	+	−	−	−	−	−	−	−	Yellow	White	*V. alginolyticus*	85.9
Sem2(2021)	Hatchery	+	+	−	−	−	−	−	−	−	Green	Turquoise	*V. vulnificus*	90.7
Sem5(2021)	Hatchery	+	+	+	−	−	−	−	−	−	Yellow	Purple	*V. cholerae*	na
AR2 (2017)	Farm	−	+	−	−	−	−	−	−	−	Yellow	White	*V. parahaemolyticus*	na
LV2 (2017)	Hatchery	−	+	−	−	−	−	−	−	−	Green	Purple	*V. parahaemolyticus*	na
CCorp (2017)	Farm	−	+	−	−	−	−	−	−	−	Green	Purple	*V. parahaemolyticus*	64.7
TLS (2017)	Farm	−	+	−	−	−	−	−	−	−	Green	Purple	*V. parahaemolyticus*	na
For10 (2017)	Farm	−	+	−	−	−	−	−	−	−	Green	Purple	*V. parahaemolyticus*	na
Vp + 418 (2016)	Farm	−	+	−	−	+	−	−	−	−	Green	Purple	*V. parahaemolyticus*	99.5
Ped (2015)	Farm	−	+	−	−	−	−	−	−	−	Yellow	White	*Serratia odorifera*	na

na bacteria not identified by the API 20E database based on its biochemical profile

[a]Code of bacterial strain and the year of isolation

[b]Luminescent strains

[c]PCR test

[d]CHROMagar *Vibrio* medium

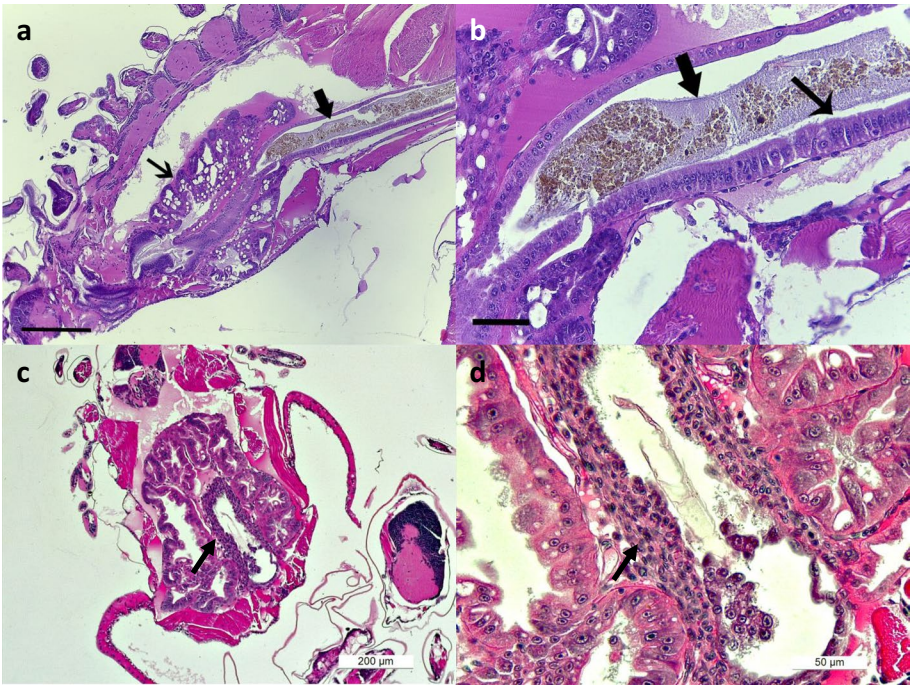

Fig. 1 **a** Histology of normal *Penaeus vannamei* larvae from an unaffected/control tank—the hepatopancreas is structurally intact (arrow), and the peritrophic membrane is complete with digested food inside (thin arrow). **b** Close-up of **a** showing the intestine and the intact peritrophic membrane (arrow). Note the normal columnar cells of the intestine (thin arrow). **c** Infiltration of hemocytes in the area surrounding the hepatopancreatic tubules (arrow). **d** Close-up of **c** showing the infiltration of hemocytes (arrow) with commencement of sloughing of hepatopancreatic epithelial cells into the lumen of the hepatopancreas. All sections are stained with H&E. Scale bars: **a**, **c** = 200 µm; **b** = 40 µm; **d** = 50 µm

Bacterial masses were present in the lumen of some, but not all, affected hepatopancreas tubules (Fig. 2d).

Molecular biology and phenotypic analysis

Table 2 provides a summary of molecular testing characterizing each isolate of bacteria based on the presence or absence of the PirAB plasmid, tox(R) gene, and the tetracycline resistant genes tet(A) to (G). Table 2 also provides a summary of some phenotypic characteristics of the isolated strains. Only one strain, Sem5, isolated in 2021, showed the presence of the tox (R), while isolate VP + 418 collected in 2015 was the only strain carrying the tet(B) gene. Biochemical-based identification using API 20E found that all strains except Sem2 and 5, both of which were isolated in 2021, were beta-galactosidase negative. Only *Vibrio* strains collected from grow-out farms could utilize citrate and ferment melibiose. The first strain isolated in 2015 was the only one found that could utilize citrate, tryptophan, inositol, sorbitol, amygdalin, and rhamnose. Three strains, Sem1, 2, and 5, were luminescent; all three, however, presented different colorations on CHROMagar. In general, there were slight differences between the strains isolated from the hatcheries and those from the farms.

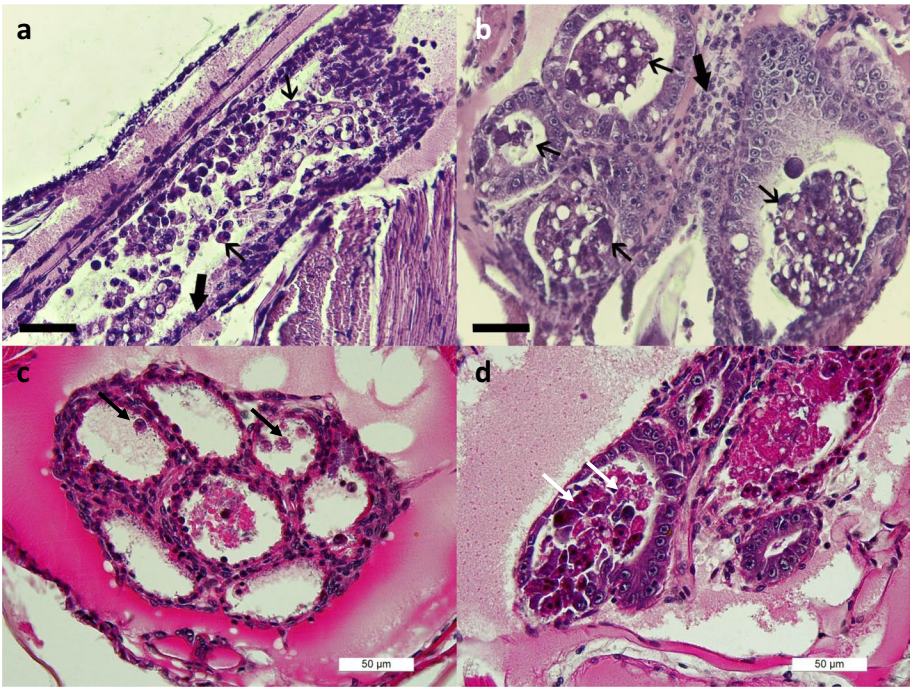

Fig. 2 **a** Intestine with a high level of sloughed cells and tissue debris (thin arrows); the intestinal epithelial cells are also affected (arrow). **b** Hepatopancreas with severe cell sloughing in the epithelium of the hepatopancreatic tubules (arrow). An infiltration of hemocytes in the area (thick arrow). **c** Moderate sloughing of cells (arrow) with the presence of hemocytic infiltration surrounding the affected hepatopancreatic tubules. **d** severe sloughing of epithelial cells into the lumen (arrow). All sections are stained with H&E. Scale bars: **a**, **b** = 40 µm; **c**, **d** = 50 µm

Microbiology

While this study places an emphasis on the pathology associated with infection, from a microbiological viewpoint, there was not a clear difference between the concentration of bacteria per gram from healthy and AHPND-affected larvae. Table 3 shows a high coefficient of variation between the samples in culture media. The only clear difference between the healthy and diseased larvae was the higher percentage of the *Vibrio* population that was found in the diseased larvae when grown on TCBS or on CHROMagar. No relationship in colony color across the isolates and culture media was found.

LC50

Table 4 shows the results of the 24-h LC50 test determined by probit analysis and the mortality rates presented in Fig. 3a, b. In general, VP418 + was more virulent in the early PL stages. Interestingly, VP + 418 did not increase during the experiment at any of the temperatures that were explored (Fig. 4a, b). In general, there was no increase between 6 and 12 h after inoculating the *Vibrio* in the flask. The cells were washed before the inoculum, and beside the organic matter generated by the algae and the excretion of the PL, there was no

Table 3 Plate count of selective media of healthy and diseased *Penaeus vannamei* larvae. A comparison of different media

	CFU/PL										
	TSA	TCBS					Chromagar				
		Yellow	Green	Total count	Luminescence	% *Vibrio*[1]	White	Purple	Turquoise	Total count	% *Vibrio*[1]
Healthy[2]59[3]	2.80E+04	1.20E+03	7.07E+01	1.30E+03	0.00E+00	4.4%	6.08E+02	1.97E+02	4.41E+01	8.48E+02	3.1%
St desv	2.90E+04	1.80E+03	1.50E+02	1.85E+03		3.4%	9.12E+02	4.06E+02	8.00E+01	1.120E+03	3.1%
% CV	105%	144%	214%	142%		79%	150%	207%	181%	132%	98%
Diseased[2]55[3]	7.04E+04	2.83E+04	4.22E+02	2.88E+04	2.34E+00	37.9%	7.90E+03	2.30E+03	2.00E+03	1.20E+04	17.7%
St desv	6.96E+04	3.07E+04	4.17E+02	3.08E+04	1.52E+01	20.1%	1.00E+04	4.80E+03	5.20E+03	1.30E+04	13.9%
% CV	99%	108%	99%	107%		53%	128%	207%	260%	102%	79%

[1]Percentage of *Vibrio* in relation to TSA count

[2]Improved from Gómez-Gil. Healthy or natural post-larvae are those that do not have luminescent bacteria; the concentration of yellow colony *Vibrio*s is less than 10^4 CFU per larvae and green *Vibrio* are less than 5% of total bacteria

[3]Number of replicates

Table 4 Summary of the 24-h LC50 probit analysis conducted on various stages of *Penaeus vannamei* challenged with VP+418. The table provides the concentration of CFU VP+418/mL required to kill 50% of the population

	PL1–2	PL3–4	PL9–10
30 °C	6.3×10^{3}	3.2×10^{4}	2.7×10^{5}
34 °C	2.2×10^{4}	1.7×10^{5}	1.0×10^{5}

organic carbon available for the *Vibrio*, which suggests that it is more likely that the *Vibrio* thrive on the feed added to the larviculture tanks.

Discussion

Vibrio is a genus of ubiquitous highly abundant bacteria in aquatic and sediment environments that can be present in high concentrations in a variety of marine organisms (Thompson et al. 2004). They can also form partnerships with zooplankton while attaching in large

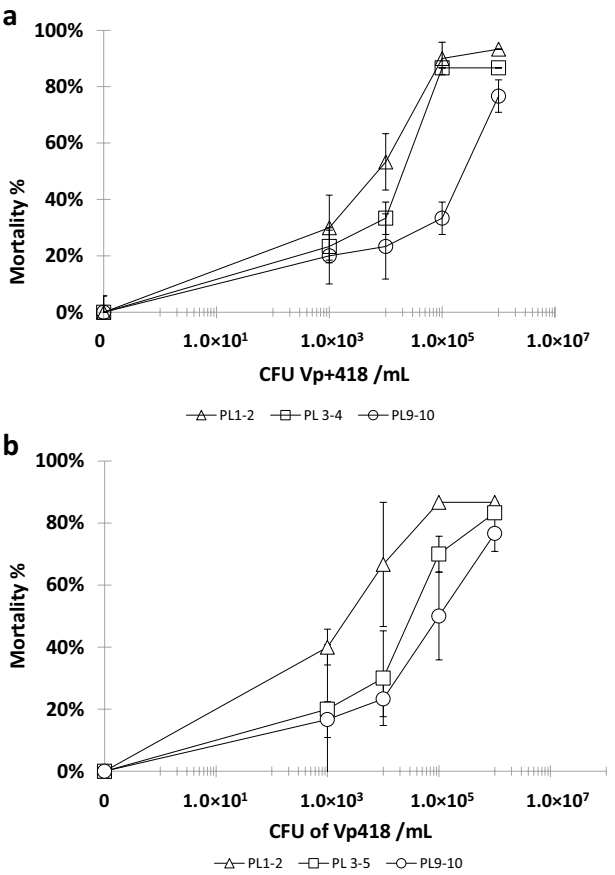

Fig. 3 Toxicity studies using different stages of *Penaeus vannamei* post-larvae (i.e., PL1-2, PL3-4, and PL 9–10) exposed to different Vp+418 concentrations. **a** At 30 °C for 24 h. **b** At 34 °C for 24 h. Each concentration represents 5 replicates

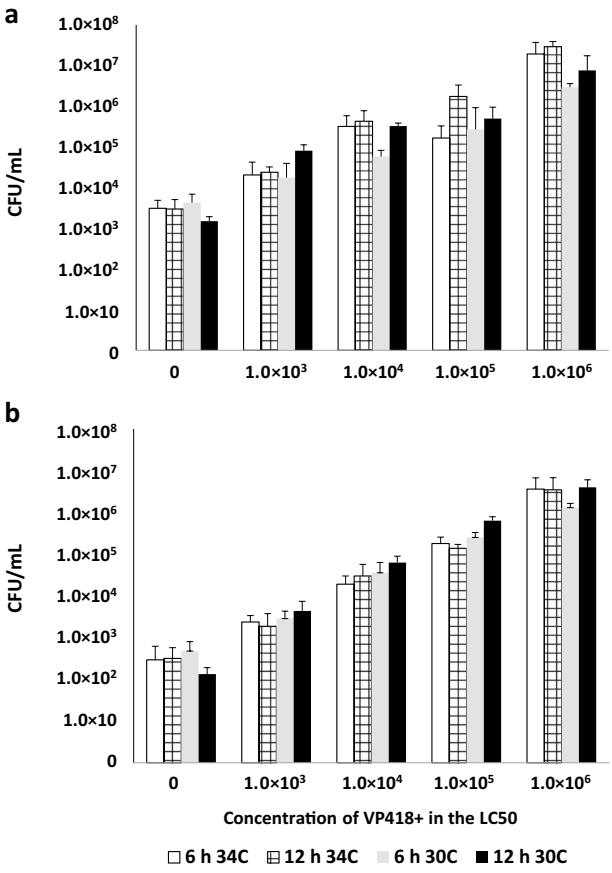

Fig. 4 **a** TSA and **b** TCBS plate counts CFU/mL sampled at 6 and 12 h after adding different concentrations of VP + 418 at 30 and 34 °C

numbers to chitinous surfaces (Heidelberg et al. 2002). Garcia and Olmos (2007) found that marine high G + C and γ-Proteobacteria were dominant on the different shrimp life sub-stages from nauplii to mysis, suggesting that they represent a large and significant fraction of the total picoplankton biomass in *P. vannamei* larval culture. In this context, *Vibrio* spp. in hatcheries can be introduced or enhanced through several pathways, for example, through infected shrimp nauplii, by contaminated water, and from microalgae, feed, *Artemia* nauplii, or contaminated farm water pipelines (Hoj et al. 2009; Yang et al. 2018; Heyse et al. 2021). The disinfection of water prior to use is a common practice in larval shrimp production, but it can lead to increased nutrient availability, reduced microbial number, lack of competition, and predation induced by the recolonization of bacteria (*r* strategists) (Hess-Erga et al. 2010). Chitin, a polymer of N-acetyl glucosamine, is a key component of the shrimp's exoskeleton; chitin-rich shrimp molts can encourage and support the growth of *Vibrio*, which can survive sub-optimal conditions and harmful environments by forming biofilms (Gode-Potratz and McCarter 2011; Nahar et al. 2012). Pathogenic bacteria levels present in the feces might also reach high numbers and eventually could reach the proper environmental conditions and produce enough toxins to cause the pathology.

Kumar et al. (2019) demonstrated that the PirAB^{VP} toxins can attach to the epithelial cells in the digestive tract of brine shrimp larvae. The intention of the present study is not

to determine the mechanisms of virulence of AHPND in larvae but to report this disease in the larvae stages. In contrast to many studies, we eliminated the toxins in the growth media by washing the cells, thus eliminating the possibility that other metabolites and toxins other than the ones produced by $PirAB^{VP}$ could enhance the mortality. According to the current study, the strain used is pathogenic to larvae and is more virulent in the initial post-larvae stages. It also showed that the population of the pathogenic *Vibrio* used in the LC50 tests did not increase. It is interesting to speculate that this *Vibrio* could not use the dissolved organic carbon of the algae or exudates of the larvae, as there was no growth after 24 h in any of the concentrations tested. The carbon source in the larvae tanks, therefore, must have come from other sources, most likely from the particulate diets used to feed the larvae.

Shrimp larvae are active filter feeders; therefore, free-living or attached bacteria may enter the stomach where bacterial toxins could be released. The microfilter in the gastric mill, which functions to filter particles down to 1 µm (Pattarayingsakul et al. 2019), is not effective in the larval stages. Until larval penaeids reach PL35, particles between 10 and 15 µm can bypass this structure (Lovett and Felder 1990), meaning that shrimp are exposed to a broad range of microorganisms, including *Vibrio* spp. bacteria (Zou et al. 2020), which can make direct contact with the hepatopancreatic epithelium (Robertson et al. 1998). It is important to stress that while *Vibrio* spp. are approximately 0.7×1.5–2.5 µm and may be able bypass the gastric mill, this passage occurs less readily in PL35 + shrimp. In addition, bacteria can also colonize the feeding apparatus and/or the rich chitin surfaces of the stomach, forming bacterial plaques in heavily infected larvae, and therefore, the mouth could become the perfect niche of pathogenic bacteria (Lavilla-Pitogo et al. 1990; Soto-Rodríguez et al. 2003; Soto-Rodríguez et al. 2006b; Soonthornchai et al. 2015). Among other factors, the extent of sloughing will depend on the concentration and strain of bacteria.

Hatcheries that reported PL-AHPND described massive and sudden mortalities, which on several occasions were observed to be within few hours. The small size and number of cells within the larval hepatopancreas is a key factor linked to the speed of the mortality event. It was not possible to repeat the timing or the exact time the mortality events occurred in some, but not all, of the cases observed (2 h), due to the fact that the bacteria in the hatchery tanks had more time (all or most of the development cycle of larval shrimp, from nauplii to PL5) to reach quorum sensing before expressing the toxin, while in the bioassay, they had a shorter time to do so. Bioassays using bacteria, however, struggle to exactly replicate the conditions found in the field, especially the dynamics of toxin production in a particular strain of bacteria and the interactions that have been described among them (Tran et al. 2020). One of the key histopathology observations in larvae affected by PL-AHPND is the lack of an intact peritrophic membrane and the presence of sloughed cells in the intestine (Fig. 2a). This histopathology is shared with zoea 2 syndrome described from hatcheries in India (Kumar et al. 2017). In contrast to this, Robertson et al. (1998) described the histopathology of "las bolitas syndrome," where the peritrophic membrane of the zoea 3 stage was reported as looking intact, while bundles of necrotic tissue form in the hepatopancreas. Bacteria were also present during the sloughing of cells in PLs affected by TPD (Zou et al. 2020; Yang et al. 2022), close to the necrotic bundles described for "las bolitas" (Robertson et al. 1998). The separation of the hepatopancreatic cells from the basal lamina in cases of vibriosis in larger-sized penaeid shrimp was described by Jiravanichpaisal et al. (1994), where the presence of invading bacteria was observed, which is a marked contrast to AHPND infections where there is a notable absence of bacteria in the hepatopancreas (Tran et al. 2013). *Vibrio* bacteria have been reported to cause detachment of cells from the midgut trunk of penaeid shrimp under experimental conditions (Martin

et al. 2004). Another interesting histopathological feature of PL-AHPND is that, occasionally, an infiltration of hemocytes is present as cell sloughing starts (see Fig. 1d), while in tubules where sloughing has resulted in a complete loss of cells, a layer of hemocytes surrounding the tubules is occasionally present (Fig. 2c). No early phase (i.e., an infiltration of hemocytes) has yet been reported for TPD. In some sections, what appeared to be bacteria colonizing the surface of the hepatopancreas was observed, and although direct confirmation of this event was not possible, this does not exclude the possibility that this can occur.

Given the small size of the larval hepatopancreas, all the tissue starts to slough from the tubules (Figs. 1d and 2b, c) and pathology does not progress from proximal to the distal area of tubules—this is a key difference in the histopathology of PL-AHPND from that described in larger-sized animals having AHPND (Tran et al. 2013). It is difficult, therefore, to find an equivalent classification in PL-AHPND to the acute, early terminal, and terminal phase for the progression of the histopathology seen for AHPND. We found two stages for larval PL-AHPND histopathology: an early and an acute-terminal phase. During the early phase, there is an infiltration of hemocytes, and the sloughing of cells starts (Fig. 1c, d); with the onset of the acute-terminal phase, massive sloughing occurs (Fig. 2b–d), while at the same time there are also, occasionally, empty tubules with few or no cells attached surrounded by an infiltration of hemocytes (Fig. 2c). These events occur in a relatively short time; the early phase could be defined only after examining numerous tissue sections and larvae. As the first samples submitted to the diagnostics laboratory were sampled from tanks just before they were discarded, it was common to observe only the tissue debris and sloughed cells in the tubule lumen along with the loss of tissue structural integrity (Fig. 2b–d), equivalent to the acute-terminal phase. As multiple individuals are prepared in tissue blocks, it is common to have partial sections from both diseased and healthy individuals in the same section. The presence of sloughed cells in the intestine (Fig. 2a) may indicate the presence of PL-AHPND; nevertheless, confirmation of the presence of the plasmids producing PirAB by PCR is always necessary.

As the dynamics of PirAB toxin–producing *Vibrios* and their interactions with other pathogenic bacteria present in the environment is strain dependent, $PirAB^{VP}$ toxins can increase the virulence of other *Vibrio* while in other cases can have no effect and work antagonistically (Tran et al. 2020). The histopathology in other similar events in larviculture might not necessarily be the same as that described here. The presence of other interacting bacteria, the speed of toxin production, and the levels and variety of the different toxins produced, might obscure some of the histopathology and progression of the phases.

The detection of the PirAB plasmid by PCR should not be considered as the only diagnostic tool for AHPND, as mutant bacteria carrying this plasmid have been described, but presenting a different histopathology in larger-sized animals to the classical one described for AHPND elsewhere (Phiwsaiya et al. 2017), and that virulence does not rely on gene copy numbers but on secreted proteins (Tinwongger et al. 2016). AHPND–causing *V. parahaemolyticus* strains have been reported to carry tetracycline resistant genes, namely tet(A) to tet(E) (Han et al. 2015; Dong et al. 2017). The present study found that beside the one tet(B)-positive strain, Vp+418, which was collected in 2015, no other strains carrying these genes have been found since. Of the 16 strains reported in this work, the Tox(R) was present in only one strain, and even though they are a wide range of culture characteristics (i.e., in colony color when grown on TCBS and on CHROMagar), it is tempting to suggest that there are very few phenotypic differences.

Shrimp larvae have different susceptibilities to the pathogenic agents produced by *Vibrio* bacteria (Goarant et al. 1998, 2000), and these agents produced by bacteria are mainly a variety of toxins (Harris and Owens 1999). The present study tests the pathogenicity of a

strain of *Vibrio* isolated in 2015 carrying the PirAB plasmid. The present work has demonstrated that AHPND can be as damaging for penaeid shrimp larviculture and the aquaculture farming business as it is for animals in the grow-out phase of production. This study demonstrates that the histopathology tentatively classified here as "PL-AHPND" differs from that in larger-sized animals in that infection is sudden and acute, i.e., in a matter of few hours on several occasions, resulting in the destruction of all hepatopancreatic epithelial cells and tubules. To determine the health of the larvae and for a correct diagnosis during routine evaluations, the industry needs to use all available tools and not only rely on plate counts and PCR.

Conclusion

This study demonstrates that: (1) the *Vibrio*s isolated from the 2015 and 2021 samples caused mortality; (2) that AHPND was detected by PCR; and (3) that sick PL displayed acute necrosis as evidenced by the H&E histopathology. Given these key points, the study concludes that there is sufficient evidence to support a strong association/causality.

Supplementary Information The online version contains supplementary material available at https://doi.org/10.1007/s10499-023-01129-0.

Acknowledgements The authors thank the editor and the anonymous referees for evaluating the manuscript and for their insightful comments.

Author contribution P.I. conceived the study and directed the research. J.E., X.H., K.A., and P.I. conducted the larval rearing and microbiology-based components of the project, A.M. performed the molecular analyses, and X.R. led the histopathology evaluation. P.I., X.R., L.F.A., and A.P.S. contributed to the interpretation of the results. X.R. took the lead in writing the manuscript in consultation with P.I., L.F.A., and A.P.S. All of the authors provided critical feedback and helped shape the research, analysis, and the manuscript text.

Data availability The datasets generated and/or analyzed during the current study are available and provided as Excel sheets in the Supplementary materials.

Declarations

Competing interests The authors declare no competing interests.

Ethics statement All research trials were conducted in strict adherence to ethical codes of practice and under the close supervision of a qualified veterinarian.

Conflict of interest The authors declare no competing interests.

References

Aguilera-Rivera D, Prieto-Davó A, Rodríguez-Fuentes G, Escalante-Herrera KS, Gaxiola G (2019) A vibriosis outbreak in the Pacific white shrimp, *Litopenaeus vannamei* reared in biofloc and clear seawater. J Invertebr Pathol 167:17246. https://doi.org/10.1016/j.jip.2019.107246

Aranguren LF, Mai HN, Noble B, Dhar AK (2020) Acute hepatopancreatic necrosis disease (VP_{AHPND}), a chronic disease in shrimp *Penaeus vannamei* population raised in Latin America. J Invertebr Pathol 174:107424. https://doi.org/10.1016/j.jip.2020.107424

Baticados MCL, Lavilla-Pitogo CR, Cruz-Lacierda ER, de la Peña LD, Suñaz NA (1990) Studies on the chemical control of luminous bacteria *Vibrio harveyi* and *V. splendidus* isolated from diseased *Penaeus monodon* larvae and rearing water. Dis Aquat Org 9:133–139. https://doi.org/10.3354/dao009133

Bell TA, Lightner DV (1988) A handbook of normal penaeid shrimp histology. The World Aquaculture Society, Baton Rouge, LA

Buller NB (2004) Bacteria from fish and animals, a practical identification manual. CABI Publishing, Cambridge, Massachusetts, USA

Cuéllar-Anjel J, Corteel M, Galli L, Alday-Sanz V, Hasson KW (2014) Principal shrimp infectious diseases, diagnosis and management. In: Alday-Sanz V (ed) The shrimp book. Nottingham University Press, UK, pp 517–622

Dangtip S, Sirikharin R, Sanguanrut P, Thitamadee S, Sritunyalucksana K, Taengchaiyaphum S, Mavichak R, Proespraiwong P, Flegel TW (2015) AP4 method for two-tube nested PCR detection of AHPND isolates of *Vibrio parahaemolyticus*. Aquacult Reports 2:158–162. https://doi.org/10.1016/j.aqrep.2015.10.002

de Souza Valente C, Wan AHL (2021) *Vibrio* and major commercially important vibriosis diseases in decapod crustaceans. J Invertebr Pathol 181:107527. https://doi.org/10.1016/j.jip.2020.107527

Dong X, Bi D, Wang H, Zou P, Xie G, Wan X, Yang Q, Zhu Y, Chen M, Guo C, Liu Z, Wang W, Huang J (2017) *pirABvp*-bearing *Vibrio parahaemolyticus* and *Vibrio campbellii* pathogens isolated from the same AHPND-affected pond possess highly similar pathogenic plasmids. Front Microbiol 8:1859. https://doi.org/10.3389/fmicb.2017.01859

Dong X, Song J, Chen J, Bi D, Wang W, Ren Y, Wang H, Wang G, Tang KFJ, Wang X, Huang J (2019) Conjugative transfer of the pVA1-type plasmid carrying the $pirAB^{vp}$ genes results in the formation of new AHPND-causing *Vibrio*. Front Cell Infect Microbiol 9:195. https://doi.org/10.3389/fcimb.2019.00195

Garcia AT, Olmos JS (2007) Quantification by fluorescent *in situ* hybridization of bacteria associated with *Litopenaeus vannamei* larvae in Mexican shrimp hatchery. Aquaculture 262:211–218. https://doi.org/10.1016/j.aquaculture.2006.10.039

Garibay-Valdez E, Martínez-Córdova LR, López-Torres MA, Almendariz-Tapia FJ, Martínez-Porchas M, Calderón K (2020) The implication of metabolically active *Vibrio* spp. in the digestive tract of *Litopenaeus vannamei* for its post-larval development. Sci Rep 10:1428. https://doi.org/10.1038/s41598-20-68222-9

Goarant C, Regnier F, Brizard R, Marteau AL (1998) Acquisition of susceptibility to *Vibrio penaeicida* in *Penaeus stylirostris* postlarvae and juveniles. Aquaculture 169:291–296. https://doi.org/10.1016/S0044-8486(98)00380-9

Goarant C, Herlin J, Brizard R, Marteau AL, Martin C, Martin B (2000) Toxic factors of *Vibrio* strains pathogenic to shrimp. Dis Aquat Org 40:101–107. https://doi.org/10.3354/dao040101

Gode-Potratz CJ, McCarter LL (2011) Quorum sensing and silencing in *Vibrio parahaemolyticus*. J Bacteriol 193:4224–4237. https://doi.org/10.1128/JB.00432-11

Gómez-Gil B, Roque A, Soto-Rodríguez S (2011) Vibriosis en camarones y su diagnóstico. Capitulo 8: 1–13. In Avances en acuicultura y manejo ambiental. Centro de Investigación en Alimentación y Desarrollo. ISBN-13: 9786071707543

Han JE, Tang KFJ, Tran LH, Lightner DV (2015) *Photorhabdus* insect-related (Pir) toxic-like genes in a plasmid of *Vibrio parahaemolyticus*, the causative agent of acute hepatopancreatic necrosis disease (AHPND) of shrimp. Dis Aquat Org 113:33–40. https://doi.org/10.3354/dao02830

Han JE, Tang KFJ, Aranguren LF, Piamsomboon P (2017) Characterization and pathogenicity of acute hepatopancreatic necrosis disease natural mutants, *pirABvp* (-) *V. parahaemolyticus*, and *pirABvp* (+) *V. campbellii* strains. Aquaculture 470:84–90. https://doi.org/10.1016/j.aquaculture.2016.12.022

Harris LJ, Owens L (1999) Production of exotoxins by two luminous *Vibrio harveyi* strains known to be primary pathogens of *Penaeus monodon* larvae. Dis Aquat Org 38:11–22. https://doi.org/10.3354/dao038011

Heidelberg JF, Heidelberg KB, Colwell RR (2002) Bacteria of the gamma-subclass Proteobacteria associated with zooplankton in Chesapeake Bay. Appl Environ Microbiol 68:5498–5507. https://doi.org/10.1128/AEM.68.11.5498-5507.2002

Hess-Erga OK, Blomvagnes-Bakke B, Vadstein (2010) Recolonization by heterotrophic bacteria after UV irradiation or ozonation of seawater; a simulation of ballast water treatment. Aquaculture 44:5439–5449. https://doi.org/10.1016/j.watres.2010.06.059

Heyse J, Props R, Kongnuan P, De Schryver P, Rombaut G, Defoirdt T, Boon N (2021) Rearing water microbiomes in white leg shrimp (*Litopenaeus vannamei*) larviculture assemble stochastically and are influenced by the microbiomes of live feed products. Environ Microbiol 23:281–298. https://doi.org/10.1111/1462-2920.15310

Hobbie JE, Daley RJ, Jasper S (1977) Use of nucleopore filters for counting bacteria by fluorescence microscopy. Appl Environ Microbiol 33:1225–1228. https://doi.org/10.1128/aem.33.5.1225-1228.1977

Hoj L, Bourne DG, Hall MR (2009) Localization, abundance, and community structure of bacteria associated with Artemia: effects of nauplii enrichment and antimicrobial treatment. Aquaculture 293:278–285. https://doi.org/10.1016/j.aquaculture.2009.04.024

Jiravanichpaisal P, Miyasaki T, Limsuwan C (1994) Histopathology, biochemistry, and pathogenicity of *Vibrio harveyi* infecting black tiger prawn *Penaeus monodon*. J Aquat Anim Health 6:27–35. https://doi.org/10.1577/1548-8667(1994)006%3c0027:HBAPOV%3e2.3.CO;2

Karunasagar I, Pai R, Malathi GR, Karunasagar I (1994) Mass mortality of *Penaeus monodon* larvae due to antibiotic-resistant *Vibrio harveyi* infection. Aquaculture 128:203–209. https://doi.org/10.1016/0044-8486(94)90309-3

Kondo H, Van PT, Dang LT, Hirono I (2015) Draft genome sequence of non- *Vibrio parahaemolyticus* acute hepatopancreatic necrosis disease strain KC13.17.5, isolated from diseased shrimp in Vietnam. Genome Announc 3(5):e00978-15. https://doi.org/10.1128/genomeA.00978-15

Kumar ST, Vidya R, Kumar S, Alavandi SV, Vijayan KK (2017) Zoea-2 syndrome of *Penaeus vannamei* in shrimp hatcheries. Aquaculture 479:759–767. https://doi.org/10.1016/j.aquaculture.2017.07.022

Kumar V, De Bels L, Couck L, Baruah K, Bossier P, Van den Broeck W (2019) PirAB^{VP} binds to epithelial cells of the digestive track and produce pathognomic AHPND lesions in germ-free brine shrimp. Toxins 11:717. https://doi.org/10.3390/toxins11120717

Lavilla-Pitogo CR, Baticados MCL, Cruz-Lacierda ER, de la Peña LD (1990) Occurrence of luminous bacterial disease of *Penaeus monodon* larvae in the Philippines. Aquaculture 91:1–13. https://doi.org/10.1016/0044-8486(90)90173-K

Lightner DV (1996) A handbook of shrimp pathology and diagnostic procedures for diseases of cultured penaeid shrimp. World Aquaculture Society, Baton Rouge, LA

López-Cervantes G, Álvarez-Ruiz P, Luna-Suárez S, Luna-González A, Esparza-Leal HM, Castro-Martínez C, Gomez-Jiménez C, Soto-Alcalá J (2021) Temperature and salinity modulate virulence and PirA gene expression of *Vibrio parahaemolyticus*, the causative agent of AHPND. Aquacult Internat 29:743–756. https://doi.org/10.1007/s10499-021-00654-0

Lovett DL, Felder DL (1990) Ontogeny of kinematics in the gut of the white shrimp *Penaeus setiferus* (Decapoda: Penaeidea). J Crust Biol 10:53–68. https://doi.org/10.1163/193724090X00249

Martin GG, Rubin N, Swanson E (2004) *Vibrio parahaemolyticus* and *V. harveyi* cause detachment of the epithelium from the midgut trunk of the penaeid shrimp *Sicyonia ingentis*. Dis Aquat Org 60:21–29. https://doi.org/10.3354/dao060021

Morales-Covarrubias MS, Cuéllar-Anjel J, Varela-Mejías A, Elizondo-Ovares C (2018) Shrimp bacterial infections in Latin America: a review. Asian Fish Sci 31S:76–87. https://doi.org/10.33997/j.afs.2018.31.s1.005

Morales-Covarrubias MS, Gómez-Gil B (2014) Enfermedades bacterianas de camarones. Guía Técnica - Patología e Inmunología de Camarones Penaeidos. OIRSA (Organizacíon Internacional Regional de Sanidad Agropecuaria), Panamá, Rep. de Panamá. pp 167–196.

Nahar S, Sultana M, Naser MN, Nair GB, Watanabe H, Ohnishi M, Yamamoto S, Endtz H, Cravioto A, Sack RB, Hasan NA, Sadique A, Huq A, Colwell RR, Alam M (2012) Role of shrimp chitin in the ecology of toxigenic *Vibrio cholerae* and cholera transmission. Front Microbiol 2:1–8. https://doi.org/10.3389/fmicb.2011.00260

Noble RT, Fuhrman JA (1998) Use of SYBR Green I for rapid epifluorescence counts of marine viruses and bacteria. Aquat Microb Ecol 14:113–118. https://doi.org/10.3354/AME014113

OIE (2019) Manual of Diagnostic Tests for Aquatic Animals. OIE, Paris

Pattarayingsakul W, Pudgerd A, Munkongwongsiri N, Vanichviriyakit R, Chaijarasphong T, Thitamadee S, Kruangkum T (2019) The gastric sieve of penaeid shrimp species is a sub-micrometer nutrient filter. J Exp Biol 222(10):jeb199638. https://doi.org/10.1242/jeb.199638

Phiwsaiya K, Charoensapsri W, Taengphu S, Dong HT, Sangsuriya P, Nguyen GTT, Pham HQ, Amparyup P, Sritunyalucksana K, Taengchaiyaphum S, Chaivisuthangkura P, Longyant S, Sithigorngul P, Senapin S (2017) A natural *Vibrio parahaemolyticus* $\Delta pirA^{Vp}$ $pirB^{Vp+}$ mutant kills shrimp but produces neither Pir^{vp} toxins nor acute hepatopancreatic necrosis disease lesions. Appl Environ Microbiol 83(16):e00680-e717. https://doi.org/10.1128/AEM.00680-17

Prachumwat A, Taengchaiyaphum S, Mungkongwongsiri N, Aldama-Cano DJ, Flegel TW, Sritunyalucksana K (2019) Update on early mortality syndrome/acute hepatopancreatic necrosis disease. J World Aquacult Soc 50:5–17. https://doi.org/10.1111/jwas.12559

Restrepo L, Bayot B, Arciniegas S, Bajaña L, Betancourt I, Panchana F, Reyes Muñoz A (2018) PirVP genes causing AHPND identified in a new *Vibrio* species (*Vibrio punensis*) within the commensal *Orientalis* clade. Sci Rep 8:13080–13080. https://doi.org/10.1038/s41598-018-30903-x

Robertson PAW, Calderon J, Carrera L, Stark JK, Zherdmand M, Austin B (1998) Experimental *Vibrio harveyi* infections in *Penaeus vannamei* larvae. Dis Aquat Org 32:151–155. https://doi.org/10.3354/dao032151

Santos HM, Tsai CY, Maquiling KRA, Tayo LL, Mariatulqabtiah AR, Lee CW, Chuang KP (2020) Diagnosis and potential treatments for acute hepatopancreatic necrosis disease (AHPND): a review. Aquacult Internat 28:169–185. https://doi.org/10.1007/s10499-019-00451-w

Shinn AP, Pratoomyot J, Griffiths D, Jiravanichpaisal J, Briggs M (2018) Asian shrimp production and the economic costs of disease. Asian Fish Sci S 31:29–58. https://doi.org/10.33997/j.afs.2018.31.S1.003

Soonthornchai W, Chaiyapechara S, Jarayabhand P, Söderhäll K, Jiravanichpaisal P (2015) Interaction of *Vibrio* spp. with the inner surface of the digestive tract of *Penaeus monodon*. PLoS ONE 10(8):e0135783. https://doi.org/10.1371/journal.pone.0135783

Soto-Rodríguez SA, Simoes N, Jones DA, Roque A, Gómez-Gil B (2003) Assessment of fluorescent labeled bacteria (FLB) for evaluation of *in vivo* uptake of bacteria (*Vibrio* spp.) by crustacean larvae. J Microbiol Methods 52:101–114. https://doi.org/10.1016/s0167-7012(02)00149-5

Soto-Rodríguez S, Armenta M, Gómez-Gil B (2006) Effects of enrofloxacin and florfenicol on survival and bacterial population in an experimental infection with luminescent *Vibrio campbellii* in shrimp larvae of *Litopenaeus vannamei*. Aquaculture 255:48–54. https://doi.org/10.1016/j.aquaculture.2005.11.035

Soto-Rodríguez SA, Simoes N, Roque A, Gómez-Gil B (2006) Pathogenicity and colonization of *Litopenaeus vannamei* larvae by luminescent vibrios. Aquaculture 258:109–115. https://doi.org/10.1016/j.aquaculture.2006.04.035

Stern S, Sonnenholzner S (2014) Semi-intensive shrimp culture: the history of shrimp farming in Ecuador. In: Alday-Sanz V (ed) The shrimp book. Nottingham University Press, UK, pp 207–232

Tang, KFJ, Bondad-Reantaso MG, Arthur JR, MacKinnon B, Hao B, Alday-Sanz V, Liang Y, Dong X (2020) Shrimp acute hepatopancreatic necrosis disease strategy manual. FAO Fisheries and Aquaculture Circular No. 1190. Rome, FAO. https://doi.org/10.4060/cb2119en

Thompson FL, Iida T, Swing J (2004) Biodiversity of *Vibrios*. Microbiol Mol Biol Rev 68:403–431. https://doi.org/10.1128/MMBR.68.3.403-431.2004

Tinwongger S, Nochiri Y, Thawonsuwan J, Nozaki R, Kondo H, Awasthi SP, Hinenoya A, Yamasaki S, Hirono I (2016) Virulence of acute hepatopancreatic necrosis disease PirAB-like relies on secreted proteins not on gene copy number. J Appl Microbiol 121:1755–1765. https://doi.org/10.1111/jam.13256

Tran LH, Nunan L, Redman RM, Mohney LL, Pantoja CR, Fitzsimmons K, Lightner DV (2013) Determination of the infectious nature of the agent of acute hepatopancreatic necrosis syndrome affecting penaeid shrimp. Dis Aquat Org 105:45–55. https://doi.org/10.3354/dao02621

Tran PTN, Kumar V, Bossier P (2020) Do acute hepatopancreatic necrosis disease-causing $PirAB^{VP}$ toxins aggravate vibriosis. Emerg Microbes Infect 19(1):1919–1932. https://doi.org/10.1080/22221751.2020.1811778

Vandenberghe J, Li Y, Verdonck L, Li J, Sorgeloos P, Xu HS, Swings J (1998) *Vibrios* associated with *Penaeus chinensis* (Crustacea: Decapoda) larvae in Chinese shrimp hatcheries. Aquaculture 169:121–132. https://doi.org/10.1016/S0044-8486(98)00319-6

Xiao J, Liu L, Ke Y, Liu Y, Pan Y, Yan S, Wang Y (2017) Shrimp AHPND-causing plasmids encoding the *pirAB* toxins as mediated by pirAB-Tn903 are prevalent in various *Vibrio* species. Sci Rep 7:42177–42177. https://doi.org/10.1038/srep42177

Yang W, Zheng C, Zheng Z, Wei Y, Lu K, Zhu J (2018) Nutrient enrichment during shrimp cultivation alters bacterioplankton assemblies and destroys community stability. Ecotox Environ Safety 156:366–374. https://doi.org/10.1016/j.ecoenv.2018.03.043

Yang F, Xu L, Huang W, Li F (2022) Highly lethal *Vibrio parahaemolyticus* strains cause acute mortality in *Penaeus vannamei* post larvae. Aquaculture 548:737605. https://doi.org/10.1016/j.aquaculture.2021.737605

Zou Y, Xie G, Jia T, Xu T, Wang C, Wan X, Li Y, Luo K, Bian X, Wang X, Kong J, Zhang Q (2020) Determination of the infectious agent of translucent post-larva disease (TPD) in *Penaeus vannamei*. Pathogens 9:741. https://doi.org/10.3390/pathogens9090741

Authors and Affiliations

Pablo Intriago[1,2] · Andres Medina[3] · Jorge Espinoza[4] · Xavier Enriquez[4] · Kelly Arteaga[3] · Luis Fernando Aranguren[5] · Andrew P. Shinn[6] · Xavier Romero[3]

Andres Medina
andresmedina2121@yahoo.com

Jorge Espinoza
jojoeh2002@yahoo.com

Xavier Enriquez
xavier_enriquez@empagran.com

Kelly Arteaga
kellyarteagav@gmail.com

Luis Fernando Aranguren
lfarangu@arizona.edu

Andrew P. Shinn
a.shinn@inveaquaculture.com

Xavier Romero
xromero2001@yahoo.com

1 South Florida Farming Corp, 13811 Old Sheridan St, Southwest Ranches, FL 33330, USA

2 Empagran S.A. ABA División Balanceado, Guayaquil, Ecuador

3 Empagran S.A, Semacua División Laboratorios, Genética E Investigación, Guayaquil, Ecuador

4 Empagran S.A, Semacua División Laboratorios, La Diablica, Anconcito, Península de Santa Elena, Ecuador

5 Aquaculture Pathology Laboratory, The University of Arizona, Tucson, AZ 85721, USA

6 Centre for Sustainable Tropical Fisheries and Aquaculture, James Cook University, Townsville, Australia